Second-Order QCD Corrections to Jet Production at Hadron Colliders: The All-Gluon Contribution

A. Gehrmann-De Ridder,[1] T. Gehrmann,[2] E. W. N. Glover,[3] and J. Pires[1]
[1]*Institute for Theoretical Physics, ETH, CH-8093 Zürich, Switzerland*
[2]*Institute for Theoretical Physics, University of Zürich, CH-8057 Zürich, Switzerland*
[3]*Institute for Particle Physics Phenomenology, University of Durham, Durham DH1 3LE, United Kingdom*
(Received 5 February 2013; published 18 April 2013)

We report the calculation of next-to-next-to-leading order QCD corrections in the purely gluonic channel to dijet production and related observables at hadron colliders. Our result represents the first next-to-next-to-leading order calculation of a massless jet observable at hadron colliders, and opens the path towards precision QCD phenomenology with the LHC.

DOI: 10.1103/PhysRevLett.110.162003 PACS numbers: 13.87.Ce, 12.38.Bx

Single inclusive jet and dijet observables are the most fundamental QCD processes measured at hadron colliders. They probe the basic parton-parton scattering in $2 \to 2$ kinematics, and thus allow for a determination of the parton distribution functions in the proton and for a direct probe of the strong coupling constant α_s up to the highest energy scales that can be attained in collider experiments.

Precision measurements of single-jet and dijet cross sections have been performed by CDF [1] and D0 [2] at the Tevatron and by ATLAS [3] and CMS [4] at the LHC. The Tevatron data are included in nearly all global fits of parton distributions, where they provide crucial information on the gluon content of the proton, and have been used to determine the strong coupling constant [5].

Theoretical predictions for these observables are accurate to next-to-leading order (NLO) in QCD [6–10] and the electroweak theory [11]. The estimated uncertainty from missing higher order corrections on the NLO QCD predictions is substantially larger than the experimental errors on single-jet and dijet data, and is thus the dominant source of error in the determination of α_s. A consistent inclusion of jet data in global fits of parton distributions is also feasible only to NLO. These theoretical limitations to precision phenomenology provide a very strong motivation for computing next-to-next-to-leading order (NNLO) corrections to jet production at hadron colliders.

At this perturbative order, three types of parton-level processes contribute to jet production: the two-loop virtual corrections to the basic $2 \to 2$ process [12], the one-loop virtual corrections to the single real radiation $2 \to 3$ process [13], and the double real radiation $2 \to 4$ process at tree level [14]. Each contribution is infrared divergent, and only their sum yields a finite and meaningful result. After ultraviolet renormalization, both virtual contributions contain explicit infrared singularities, which are compensated by infrared singularities from single or double real radiation. These become explicit only after integrating out the real radiation contributions over the phase space relevant to single-jet or dijet production. This interplay with the jet definition complicates the extraction of infrared singularities from the real radiation process. It is typically done by subtracting an infrared approximation from the corresponding matrix elements. These infrared subtraction terms are sufficiently simple to be integrated analytically, such that they can be combined with the virtual contributions to obtain the cancellation of all infrared singularities. Several generic methods for the construction of subtraction terms are available at NLO [15–17].

The development of subtraction methods for NNLO calculations is a very active field of research. Up to now, various methods were constructed and applied to specific NNLO calculations of exclusive observables: sector decomposition [18] applied to Higgs production [19] and vector boson production [20]; q_T subtraction [21] to Higgs production [22], vector boson production [23], associated VH production [24], photon pair production [25] and top quark decay [26]; antenna subtraction [27] to three-jet production [28,29] and related event shapes [30,31] in e^+e^- annihilation; and sector-improved residue subtraction [32] to top quark pair production [33].

The antenna subtraction method [27,34,35] constructs subtraction terms from antenna functions which encapsulate all unresolved radiation in between a pair of hard radiator partons. At NNLO, antenna functions with up to two unresolved partons at tree level and one unresolved parton at one loop are required. For hadron collider observables, one [36] or both [37,38] radiator partons can be in the initial state.

For the NNLO all-gluon contribution to jet production at hadron colliders, the antenna subtraction terms were constructed for the tree-level double real radiation process in Ref. [39] and for the one-loop single real radiation process in Ref. [40]. These subtraction terms were integrated and combined [41] with the relevant two-loop matrix elements and parton distributions, resulting in a full cancellation of infrared poles. We have now implemented these terms into a parton-level event generator, which can compute the all-gluon contribution to any infrared-safe observable related

 © 2013 American Physical Society

to dijet final states at hadron colliders to NNLO accuracy. The program consists of three integration channels:

$$d\sigma_{gg,\mathrm{NNLO}} = \int_{d\Phi_4} [d\sigma^{RR}_{gg,\mathrm{NNLO}} - d\sigma^{S}_{gg,\mathrm{NNLO}}] + \int_{d\Phi_3} [d\sigma^{RV}_{gg,\mathrm{NNLO}} - d\sigma^{T}_{gg,\mathrm{NNLO}}] + \int_{d\Phi_2} [d\sigma^{VV}_{gg,\mathrm{NNLO}} - d\sigma^{U}_{gg,\mathrm{NNLO}}], \quad (1)$$

where each of the square brackets is finite and well behaved in the infrared singular regions. For the all-gluon channel, the construction of the three subtraction terms $d\sigma^{S,T,U}_{ij,\mathrm{NNLO}}$ was described in Refs. [39–41].

In the three-parton and four-parton channel, the phase space has been decomposed into multiple wedges (6 three-parton wedges and 30 four-parton wedges), each containing only a subset of possible infrared singular contributions. Inside each wedge, the generation of multiple phase space configurations related by angular rotation of unresolved pairs of particles around their common momentum axis ensures a local convergence of the antenna subtraction term to the relevant matrix element. Owing to the symmetry properties of the all-gluon final state, many wedges yield identical contributions, thereby allowing a substantial speed up of their evaluation.

Jets in hadronic collisions can be produced through a variety of different partonic subprocesses, and the all-gluon process is only one of them. Our results on this process cannot therefore be directly compared with experimental data. The all-gluon process does, however, allow us to establish the calculational method, and to qualify the potential impact of NNLO corrections on jet observables. It should be noted that the NLO corrections to hadronic two- and three-jet production were also first derived in the all-gluon channel [42–44], well before full results could be completed [6–8]. In both cases, the all-gluon results were extremely vital both for establishing the methodology and for assessing the infrared sensitivity of different jet algorithms [44].

Our numerical studies for proton-proton collisions at center-of-mass energy $\sqrt{s} = 8$ TeV concern the single-jet inclusive cross section (where every identified jet in an event that passes the selection cuts contributes, such that a single event potentially enters the distributions multiple times) and the two-jet exclusive cross section (where events with exactly two identified jets contribute).

Jets are identified using the anti-k_T algorithm with the resolution parameter $R = 0.7$. Jets are accepted at central rapidity $|y| < 4.4$, and ordered in transverse momentum. An event is retained if the leading jet has $p_{T1} > 80$ GeV. For the dijet invariant mass distribution, a second jet must be observed with $p_{T2} > 60$ GeV.

All calculations are carried out with the MSTW08NNLO gluon distribution function [45], including the evaluation of

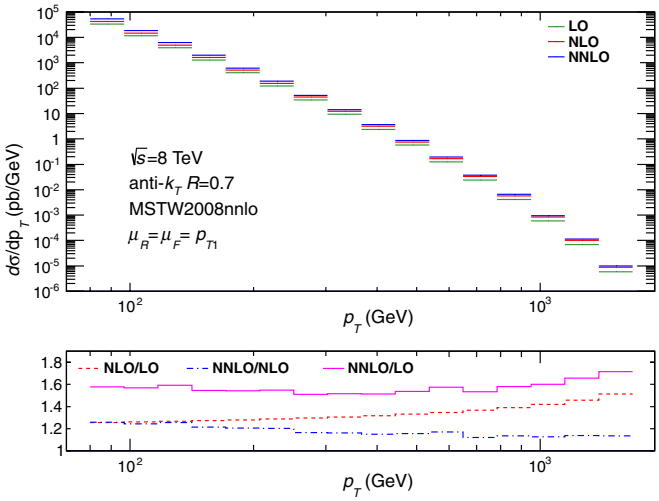

FIG. 1 (color online). Inclusive jet transverse energy distribution $d\sigma/dp_T$ for jets constructed with the anti-k_T algorithm with $R = 0.7$ and with $p_T > 80$ GeV, $|y| < 4.4$, and $\sqrt{s} = 8$ TeV at NNLO (blue), NLO (red), and LO (dark green). The lower panel shows the ratios of NNLO, NLO, and LO cross sections.

the LO and NLO contributions [46]. This choice of parameters allows us to quantify the size of the genuine NNLO contributions to the parton-level subprocess. Factorization and renormalization scales (μ_F and μ_R) are chosen dynamically on an event-by-event basis. As the default value, we set $\mu_F = \mu_R \equiv \mu$ and set μ equal to the transverse momentum of the leading jet so that $\mu = p_{T1}$.

In Fig. 1 we present the inclusive jet cross section for the anti-k_T algorithm with $R = 0.7$ and with $p_T > 80$ GeV and $|y| < 4.4$ as a function of the jet p_T at LO, NLO, and NNLO, for the central scale choice $\mu = p_{T1}$. The NNLO/NLO k factor shows the size of the higher order NNLO

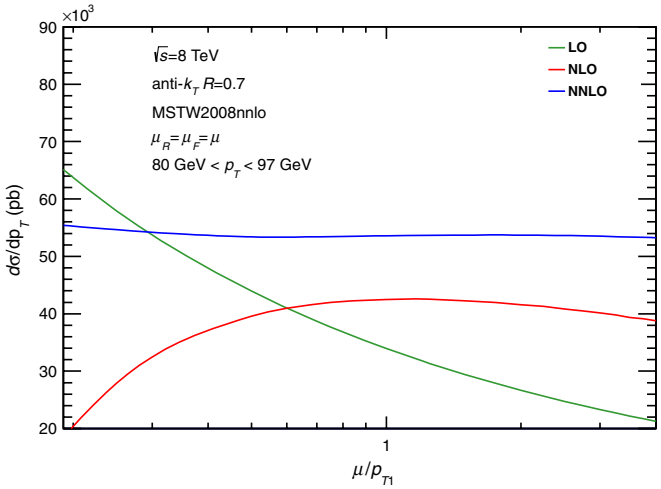

FIG. 2 (color online). Scale dependence of the inclusive jet cross section for pp collisions at $\sqrt{s} = 8$ TeV for the anti-k_T algorithm with $R = 0.7$ and with $|y| < 4.4$ and 80 GeV $< p_T <$ 97 GeV at NNLO (blue), NLO (red), and LO (green).

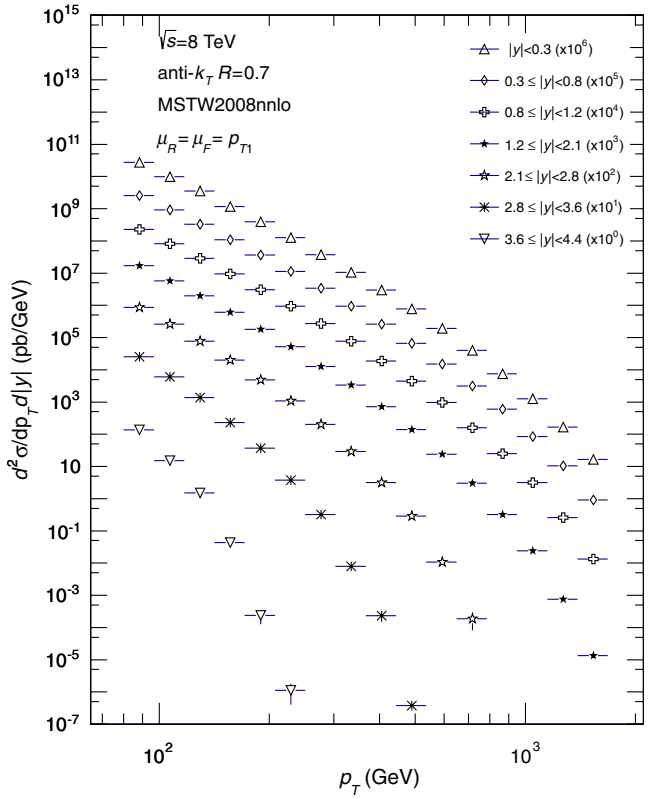

FIG. 3 (color online). The doubly differential inclusive jet transverse energy distribution $d^2\sigma/dp_T d|y|$ at $\sqrt{s} = 8$ TeV for the anti-k_T algorithm with $R = 0.7$ and for $E_T > 80$ GeV and various $|y|$ slices.

effect to the cross section in each bin with respect to the NLO calculation. For this scale choice we see that the NNLO/NLO k factor is approximately flat across the p_T range corresponding to a 15%–25% increase compared to the NLO cross section.

One of the main motivations for computing the NNLO QCD corrections is to reduce the scale uncertainty in the theoretical prediction. This is illustrated in Fig. 2 for the single-jet inclusive cross section for jets with $|y| < 4.4$ and 80 GeV $< p_T <$ 97 GeV. We see that the scale dependence of the cross section at NNLO is vastly reduced. The scale dependence of other p_T and y slices is also reduced.

To illustrate the range of observables that can be studied with our computation we show in Fig. 3 the inclusive jet cross section in double-differential form in jet p_T and rapidity bins at NNLO. The p_T range is divided into 16 jet p_T bins and seven rapidity intervals over the range 0.0–4.4 covering central and forward jets.

Figure 4 shows the double-differential k factors for the distribution in Fig. 3 for three rapidity slices: $|y| < 0.3$, $0.3 < |y| < 0.8$, and $0.8 < |y| < 1.2$. We observe that the NNLO correction increases the cross section between 25% at low p_T to 12% at high p_T with respect to the NLO calculation and this behavior is similar for all three rapidity slices.

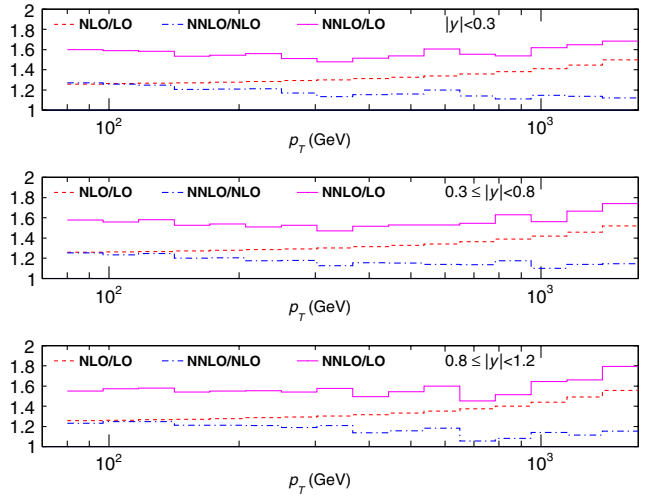

FIG. 4 (color online). Double differential k factors for $p_T >$ 80 GeV and three $|y|$ slices: $|y| < 0.3$, $0.3 < |y| < 0.8$, and $0.8 < |y| < 1.2$.

As a final observable, we computed the dijet cross section as a function of the dijet mass at NNLO. This is shown in Fig. 5 for the scale choice $\mu = 2p_{T1}$ together with the LO and NLO results. The dijet mass is computed from the two jets with the highest p_T and $|y_1|$, $|y_2| < 4.4$ with y^*, defined as half the rapidity difference of the two leading jets $y^* = |y_1 - y_2|/2 < 0.5$. We see that the NNLO/NLO k factor is approximately flat across the m_{jj} range corresponding to a 15%–20% increase compared to the NLO cross section.

In conclusion, we have described the first calculation of the fully differential inclusive jet and dijet cross sections

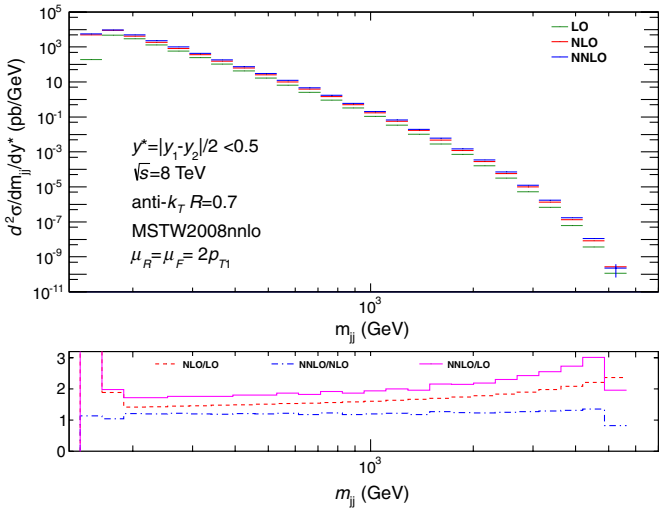

FIG. 5 (color online). Exclusive dijet invariant mass distribution $d\sigma/dm_{jj}dy^*$ at $\sqrt{s} = 8$ TeV for $y^* < 0.5$ with $p_{T1} >$ 80 GeV, $p_{T2} > 60$ GeV, and $|y_1|$, $|y_2| < 4.4$ at NNLO (blue), NLO (red), and LO (dark green). The lower panel shows the ratios of NNLO, NLO, and LO cross sections.

at hadron colliders at NNLO in the strong coupling constant using the new parton-level generator NNLOJET. We have considered the NNLO QCD corrections from the purely gluonic channel at leading color. As demonstrated in Refs. [40,41], using the antenna subtraction scheme the explicit ϵ poles in the dimension regularization parameter of one- and two-loop matrix elements entering this calculation are cancelled in analytic and local form against the ϵ poles of the integrated antenna subtraction terms, thereby enabling the computation of jet cross sections at hadron colliders at NNLO accuracy. All of these techniques can be readily applied to the quark contributions.

For all of the observables considered here, we observed a dramatic reduction of the respective uncertainties in the theory prediction due to variations of the factorization and renormalization scales. We expect similar conclusions when including the processes involving quarks.

This research was supported in part by the UK Science and Technology Facilities Council, in part by the Swiss National Science Foundation (SNF) under Contracts No. PP00P2-139192 and No. 200020-138206, and in part by the European Commission through the "LHCPhenoNet" Initial Training Network PITN-GA-2010-264564. E .W .N .G. gratefully acknowledges the support of the Wolfson Foundation, the Royal Society, and the Pauli Center for Theoretical Studies.

[1] T. Aaltonen *et al.* (CDF Collaboration), Phys. Rev. D **78**, 052006 (2008).
[2] V. M. Abazov *et al.* (D0 Collaboration), Phys. Rev. Lett. **101**, 062001 (2008).
[3] G. Aad *et al.* (ATLAS Collaboration), Eur. Phys. J. C **71**, 1512 (2011); Phys. Rev. D **86**, 014022 (2012).
[4] S. Chatrchyan *et al.* (CMS Collaboration), Phys. Lett. B **700**, 187 (2011); Phys. Rev. Lett. **107**, 132001 (2011); J. High Energy Phys. 06 (2012) 036; S. Chatrchyan *et al.* (CMS Collaboration), arXiv:1212.6660.
[5] V. M. Abazov *et al.* (D0 Collaboration), Phys. Rev. D **80**, 111107 (2009).
[6] S. D. Ellis, Z. Kunszt, and D. E. Soper, Phys. Rev. Lett. **69**, 1496 (1992).
[7] W. T. Giele, E. W. N. Glover, and D. A. Kosower, Phys. Rev. Lett. **73**, 2019 (1994).
[8] Z. Nagy, Phys. Rev. Lett. **88**, 122003 (2002); Phys. Rev. D **68**, 094002 (2003).
[9] S. Alioli, K. Hamilton, P. Nason, C. Oleari, and E. Re, J. High Energy Phys. 04 (2011) 081.
[10] J. Gao, Z. Liang, D. E. Soper, H.-L. Lai, P. M. Nadolsky, and C.-P. Yuan, Comput. Phys. Commun. **184**, 1626 (2013).
[11] S. Dittmaier, A. Huss, and C. Speckner, J. High Energy Phys. 11 (2012) 095.
[12] E. W. N. Glover, C. Oleari, and M. E. Tejeda-Yeomans, Nucl. Phys. **B605**, 467 (2001); E. W. N. Glover and M. Tejeda-Yeomans, J. High Energy Phys. 05 (2001) 010; Z. Bern, A. De Freitas, and L. J. Dixon, J. High Energy Phys. 03 (2002) 018.
[13] Z. Bern, L. J. Dixon, D. C. Dunbar, and D. A. Kosower, Nucl. Phys. **B425**, 217 (1994).
[14] M. L. Mangano and S. J. Parke, Phys. Rep. **200**, 301 (1991).
[15] S. Frixione, Z. Kunszt, and A. Signer, Nucl. Phys. **B467**, 399 (1996).
[16] S. Catani and M. H. Seymour, Nucl. Phys. **B485**, 291 (1997).
[17] D. A. Kosower, Phys. Rev. D **57**, 5410 (1998).
[18] T. Binoth and G. Heinrich, Nucl. Phys. **B585**, 741 (2000); Nucl. Phys. **B693**, 134 (2004); C. Anastasiou, K. Melnikov, and F. Petriello, Phys. Rev. D **69**, 076010 (2004).
[19] C. Anastasiou, K. Melnikov, and F. Petriello, Phys. Rev. Lett. **93**, 262002 (2004); C. Anastasiou, G. Dissertori, and F. Stöckli, J. High Energy Phys. 09 (2007) 018; C. Anastasiou, F. Herzog, and A. Lazopoulos, J. High Energy Phys. 03 (2012) 035.
[20] K. Melnikov and F. Petriello, Phys. Rev. D **74**, 114017 (2006).
[21] S. Catani and M. Grazzini, Phys. Rev. Lett. **98**, 222002 (2007).
[22] M. Grazzini, J. High Energy Phys. 02 (2008) 043.
[23] S. Catani, L. Cieri, G. Ferrera, D. de Florian, and M. Grazzini, Phys. Rev. Lett. **103**, 082001 (2009); S. Catani, G. Ferrera, and M. Grazzini, J. High Energy Phys. 05 (2010) 006.
[24] G. Ferrera, M. Grazzini, and F. Tramontano, Phys. Rev. Lett. **107**, 152003 (2011).
[25] S. Catani, L. Cieri, D. de Florian, G. Ferrera, and M. Grazzini, Phys. Rev. Lett. **108**, 072001 (2012).
[26] J. Gao, C. S. Li, and H. X. Zhu, Phys. Rev. Lett. **110**, 042001 (2013).
[27] A. Gehrmann-De Ridder, T. Gehrmann, and E. W. N. Glover, J. High Energy Phys. 09 (2005) 056.
[28] A. Gehrmann-De Ridder, T. Gehrmann, E. W. N. Glover, and G. Heinrich, J. High Energy Phys. 11 (2007) 058; Phys. Rev. Lett. **100**, 172001 (2008).
[29] S. Weinzierl, Phys. Rev. Lett. **101**, 162001 (2008); J. High Energy Phys. 07 (2009) 009; Eur. Phys. J. C **71**, 1565 (2011).
[30] A. Gehrmann-De Ridder, T. Gehrmann, E. W. N. Glover, and G. Heinrich, J. High Energy Phys. 12 (2007) 094.
[31] S. Weinzierl, J. High Energy Phys. 06 (2009) 041.
[32] M. Czakon, Phys. Lett. B **693**, 259 (2010); Nucl. Phys. **B849**, 250 (2011).
[33] P. Barnreuther, M. Czakon, and A. Mitov, Phys. Rev. Lett. **109**, 132001 (2012); M. Czakon and A. Mitov, J. High Energy Phys. 12 (2012) 054; J. High Energy Phys. 01 (2013) 080.
[34] A. Daleo, T. Gehrmann, and D. Maitre, J. High Energy Phys. 04 (2007) 016.
[35] J. Currie, E. W. N. Glover, and S. Wells, arXiv:1301.4693.
[36] A. Daleo, A. Gehrmann-De Ridder, T. Gehrmann, and G. Luisoni, J. High Energy Phys. 01 (2010) 118.
[37] R. Boughezal, A. Gehrmann-De Ridder, and M. Ritzmann, J. High Energy Phys. 02 (2011) 098; A. Gehrmann-De Ridder, T. Gehrmann, and M. Ritzmann, J. High Energy Phys. 10 (2012) 047.
[38] T. Gehrmann and P. F. Monni, J. High Energy Phys. 12 (2011) 049.
[39] E. W. N. Glover and J. Pires, J. High Energy Phys. 06 (2010) 096.

[40] A. Gehrmann-De Ridder, E. W. N. Glover, and J. Pires, J. High Energy Phys. 02 (2012) 141.
[41] A. Gehrmann-De Ridder, T. Gehrmann, E. W. N. Glover, and J. Pires, J. High Energy Phys. 02 (2013) 026.
[42] S. D. Ellis, Z. Kunszt, and D. E. Soper, Phys. Rev. Lett. **62**, 726 (1989); S. D. Ellis, Z. Kunszt, and D. E. Soper, Phys. Rev. D **40**, 2188 (1989).
[43] Z. Trocsanyi, Phys. Rev. Lett. **77**, 2182 (1996).
[44] W. B. Kilgore and W. T. Giele, Phys. Rev. D **55**, 7183 (1997).
[45] A. D. Martin, W. J. Stirling, R. S. Thorne, and G. Watt, Eur. Phys. J. C **63**, 189 (2009).
[46] Note that the evolution of the gluon distribution within the PDF set together with the value of α_s intrinsically includes contributions from the light quarks. The NNLO calculation presented here is "gluons-only" in the sense that only gluonic matrix elements are involved.